International Journal of GEOMATE, Oct. 2023, Vol. 25, Issue 110, pp.98-105
ISSN: 2186-2982 (P), 2186-2990 (O), Japan, DOI: https://doi.org/10.21660/2023.110.3975
Geotechnique, Construction Materials and Environment

BEHAVIOUR OF RC FRAME USING PRECAST FOAM CONCRETE STRENGTHENED WITH CFRP AS AN INFILL WALL UNDER HORIZONTAL CYCLIC LOADING

Yohans Sunarno[1], Muhammad Wihardi Tjaronge[1], Rita Irmawaty[1] and Achmad Bakri Muhiddin[1*]

[1]Civil Engineering Department, Hasanuddin University, Makassar, South Sulawesi, Indonesia

*Corresponding Author, Received: 9 June 2023, Revised: 17 July 2023, Accepted: 20 July 2023

ABSTRACT: An experimental study was undertaken to examine the behavior of RC-frames employing precast foam concrete reinforced with diagonal CFRP as an infill wall under ASTM E2126-02a cycle testing methodology (ASTM 2003) in order to anticipate the onset of earthquake-related disasters. The study aimed to determine the failure rate and mechanism based on FEMA 356. An RC frame with precast foam concrete acting as an infill wall without retrofitting (WTI) and an RC frame with precast foam concrete acting as an infill wall and CFRP retrofitting at a width of 36 cm (WTC) were constructed as two different types of examples. The results showed that whereas the WTI produced a maximum load value of 44.88 kN at push loading and 52.30 kN at pull loading, the WTC produced a maximum load value of 102.87 kN at push loading and 80.09 kN at pull loading. The diagonal CFRP retrofitting increased the RC frame's capacity to support in-plane horizontal cyclic stresses when foam concrete precast was used as an infill wall. The test specimen with the CFRP retrofitting underwent a shear failure that started with the CFRP strip debonding and ended with a shear structural collapse. The infill wall had an in-plane failure and a diagonal crack with shear collapse. This demonstrates that the maximum load that the RC specimen could withstand after being retrofitted with CFRP rose for each structural performance grade.

Keywords: Behavior, CFRP, Precast foam concrete, Horizontal cyclic loading, Building performance grade

1. INTRODUCTION

Earthquakes are extremely hazardous and cause widespread destruction to buildings and structures. Although there is currently no known method to prevent their occurrence [1-3], steps are being taken to reduce their effects. One such step is the improvement of the structural aspects of buildings, with a particular focus on the reinforced concrete frames and walls. This approach involves implementing correct and safe structural design plans that can anticipate the horizontal and cyclic loads associated with earthquakes [4].

To ensure earthquake-resistant structures, various engineering practices and technologies have been developed and implemented to ensure structural retrofitting in the construction system. These practices include the application of different retrofitting techniques, such as infill wall systems in reinforced concrete (RC) frames, prefabricated panels, steel bracing, and concrete covering in RC frames. Among these techniques, infill frames are considered the most practical reinforcement method for low-to-intermediate grade reinforced concrete buildings worldwide. This is due to their ability to increase the horizontal load rate of the RC frame system, reduce the drift caused by the maximum load, improve global rigidity, horizontal strength, and energy dissipation capacity, and avoid column shear collapse [5]. Several investigational studies have been conducted on infill RC frames, and they have shown remarkable improvements in the global system feature. For instance, Hashemi and Mosallam [6] tested the rocking table of the RC frame with an infill wall and demonstrated almost four times improvement in the stiffness of the structural system, a reduction in the period by almost half, and an increase in the damping coefficient in the range of 4-6% to 12%.

The main criteria for selecting a material for an ideal infill wall is lightweight and sufficient strength. An example of lightweight concrete (LC) with the ability to enhance the overall seismic feature of RC frames is foam concrete. The enhancement is usually associated with the light self-weight of the material as well as the ability to reduce subsequent disasters linked to the wall damage while focusing on the structural system feature in terms of strength and ductility. It is pertinent to note that lightweight concrete normally has good seismic performance with a small density and modulus of elasticity due to its production through a porous structure containing bubbles. Previous studies have already shown that Autoclaved Aerated Concrete (AAC) is closer to an ideal infill wall for frame structures compared to gypsum bricks and panels [4]. Moreover, foam concrete is a slurry mortar normally produced using sand, cementitious material, water, and foam agents, and its density ranges from 400 to 1,850 kg/m3. There are usually randomly distributed bubbles in its mixture, and the concrete is characterized by high flowability, less cement usage, and more efficient aggregate application. The application of foam concrete as infill walls in RC frames has the ability to reduce the weight of the frame, and this has a valuable influence on structural global performance [7-11].

Fiber-Reinforced Polymers (FRP) are the right alternative material to be used for retrofitting and reinforcement due to their thin thickness and relatively easy application. According to the American Concrete Institute (ACI) [1], FRP is a general term for composite materials consisting of a polymer substance that is reinforced by fibrous ingredients such as fabrics, sheets, strands, or other forms of fibers. An example of these is carbon fiber-reinforced polymers (CFRP), which involve using carbon fiber for reinforcement and ordinarily use polymer resins for their matrices and apply epoxy-pattern to bind the reinforcements together. It is important to note that the characterization of CFRPs is normally influenced by two different components, and these include the lightweight and durability under several environmental conditions as well as the superior strength compared to other ordinary materials. The lightweight attribute facilitates the easier application of this material, even in limited spaces, without the need for large equipment. It also has the ability to improve the strength and stiffness of the structural system using a very small mass, and this is considered very beneficial from the seismic perspective [1]. Several analytical studies proved that CFRP retrofitting can significantly enhance the strength and ductility of structural components without increasing the stiffness [12, 13]. This indicates its suitability to anchor reinforced concrete columns and beams due to its high elasticity modulus and strength. CFRP also has good resistance against corrosion and environmental conditions, thereby increasing its popularity for the reinforcement of RC structures using different types and sizes available in the market. Therefore, several investigations have been conducted on its application in retrofitting RC components as well as to analyze its behavior.

Previous studies on the application of CFRP in reinforcing concrete components have identified three main modes of failure, which are debonding of concrete components, epoxy failure due to greater shear stress compared to epoxy shear strength, and CFRP rupture under high axial voltage load [14-18]. However, it is rare to have CFRP rupture caused by the tensile axial load in the field due to the material's high axial tensile strength. In most cases, the limit of shear stress leads to the collapse of CFRP debonding from the concrete cover or concrete-adhesive interzone before rupture. The most common rupture pattern is the debonding from the concrete cover. To assess the failure mechanisms associated with the structural components of specimens, this study employed the Federal Emergency Management Agency (FEMA) 356 standard [19]. The standard links building performance grades to the status of damage and identify the consequences in relation to the post-earthquake viability of the building for the occupants. This includes the capacity to resume normal functions, the feasibility of living in the house after the earthquake, as well as the risks and guarantee of safety for the lives in the area.

2. RESEARCH SIGNIFICANCE

This study discusses the application of foam concrete as infill wall material in reinforced concrete frames for medium-sized buildings in anticipation of horizontal lateral loads due to earthquakes. Diagonal CFRP retrofitting bonded to the precast foam concrete as an infill wall is expected to increase the lateral capacity of the reinforced concrete frame. The grade of failure that occurred was evaluated using FEMA 356 standards. From this research, it is hoped that it can provide additional insights into the use of lightweight composite materials that are able to withstand horizontal lateral loads due to earthquakes with measurable levels of failure.

3. DESCRIPTION OF SPECIMENS

To analyze the behavior of reinforced concrete (RC) walls, this study conducted experimentation of specimens designed at a 1:1 scale with two different variations. The first variation, an RC frame with precast foam concrete as an infill wall without CFRP retrofitting (WTI), compared to the second variation involved an RC frame with precast foam concrete and diagonal CFRP retrofitting with a width of 36 cm (WTC). The goal of this experimentation was to investigate the behavior of the walls under the cyclic testing protocol of ASTM E2126-02a (ASTM 2003) [20], the effect of the diagonal CFRP retrofitting on precast foam concrete as an infill wall, as well as the failure rates and mechanisms based on FEMA 356 standards.

3.1 Material Properties

Tables 1, 2, and 3 show the properties of all materials used in this study, including concrete, mortar, reinforcing bars, and CFRP. It is significant to note that the concrete used consists of precast foam concrete, mortar, column, as well as bottom and upper beams. Testing the characteristics of each of these materials using applicable international standards.

Table 1 Compressive strength of materials used

Material	Compressive Strength (MPa)	ASTM Method
Foam concrete	2.29	ASTM C39
Mortar	5.20	ASTMC780
Bottom beam	22.60	ASTM C39
Column	30.25	ASTM C39
Upper beam	30.25	ASTM C39

Table 2 Mechanical properties of reinforcing bars

Dia.	Stress (Mpa) Yield Strength	Stress (Mpa) Ultimate Tensile Strength	Classification
D13	474.748	642.175	BJTS 520
Ø8	378.460	419.896	BJTP 280

Table 3 Mechanical properties of CFRP composite

Description	Result	ASTM Method
Thickness (mm)	1.00	-
Tensile strength (MPa)	834	D3039
Tensile modulus (MPa)	82000	D3039
Ultimate tensile strain (%)	0.85	D790

3.2 Specimen Type

The matrix of specimens consisting of RC frames having precast foam concrete infill walls with and without CFRP retrofitting produced on a 1:1 scale is presented in the following Table 4 as well as Figures 1 and 2.

Table 4 Variations of the specimens

Specimen	Code
RC frame with precast foam concrete as an infilled wall without CFRP	WTI
RC frame with precast foam concrete as an infilled wall with diagonal CFRP retrofitting at a width of 36 cm	WTC

3.3 CFRP Application

The process of installing diagonal CFRP strips to reinforce the foam concrete infill wall, as shown in Figure 3, involved several stages. The primary objective of CFRP usage was to increase the wall's stiffness and resistance to horizontal forces. The process began with cleaning and smoothing the surface of the wall, epoxy, CFRP, and anchor application and then drawing the failure scheme grid.

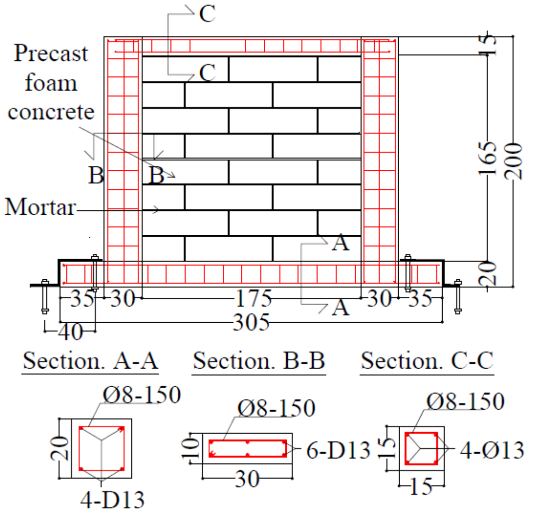

Fig. 1 WTI specimen

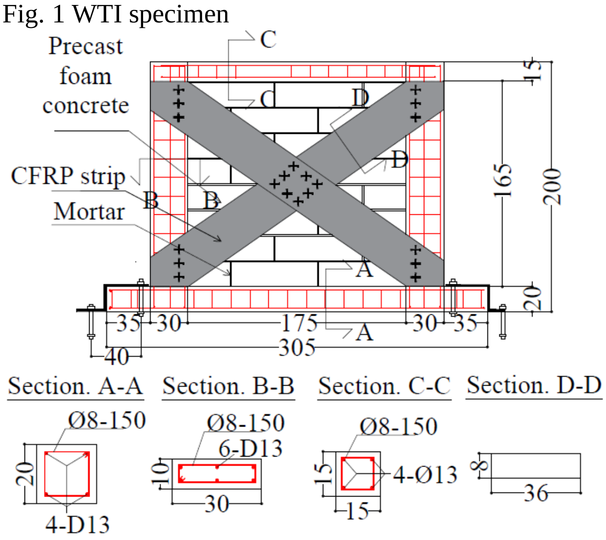

Fig. 2 WTC specimen

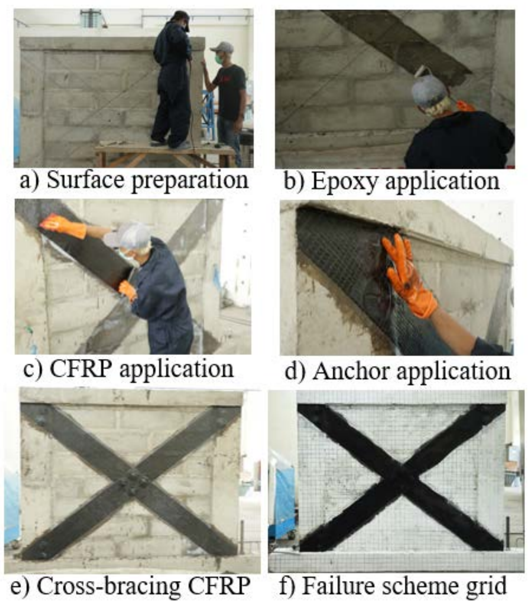

Fig. 3 CFRP application

3.4. Horizontal Cyclic Loading

Horizontal cyclic loading was applied on both specimens using ASTM E2126-02a (ASTM 2003) guidelines with the B (*ISO 16670 Protocol*) method. The setup for the RC frame with precast foam concrete as an infill wall specimen is presented in the following Figure 4.

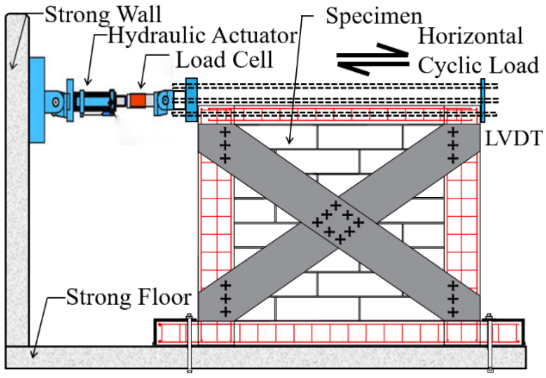

Fig. 4 Setting up of the cyclic load.

A set of hydraulic actuators was provided to function as cyclic loads and as cells to apply loads to the sliding walls. Moreover, the cyclic loads were applied under controlled displacement conditions where Δm was defined based on the horizontal deformation of RC specimen height by 2% according to the building planning rules of SNI 1726-2019 [25]. The Δm value was recorded to be 40 mm because the specimen height used was 2,000 mm. A displacement-controlled loading procedure was also applied by grouping the displacement cycles in phases based on the gradual increase in their rates. The ISO loading is indicated in the following Table 5 and Figure 5.

Table 5 Loading schedule [20]

Mode	Step	Min. amount of cycle	Amplitude, % Δ_m	Drift Ratio %
1	1	1	1.25	0.025
	2	1	2.50	0.05
	3	1	5.00	0.10
	4	1	7.50	0.15
	5	1	10.00	0.20
2	6	3	20.00	0.40
	7	3	40.00	0.80
	8	3	60.00	1.20
	9	3	80.00	1.60
	10	3	100.00	2.00
	11	3	Add. increments of 20 (until failure	2.40

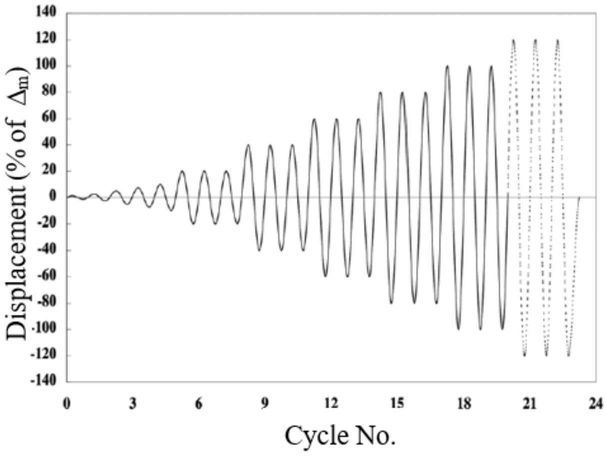

Fig. 5 Loading schedule [20]

4. BUILDING PERFORMANCE GRADE

Federal Emergency Management Agency (FEMA) 356 standard [19] provides the correlation between the structural performance grade of a building and the status of damage to the perpendicular components of the horizontal force restraint system. Moreover, the building performance grade was determined based on the integrity of the structural and non-structural components. It is important to note that the four structural performance grades evaluated include Immediate Occupancy (S-1), Life Safety (S-3), Collapse Prevention (S-5), and Not Considered (S-6). These were in addition to the two grades of intermediate structural performance, which include the Damage Control scope (S-2) and Limited Safety scope (S-4).

5. RESULTS AND DISCUSSION

5.1 WTI Frame

Figure 6 presents the relationship of load to displacement in the form of a hysteresis loop curve after horizontal cyclic load was applied to WTI specimens. The compressive loading curve indicates a notable improvement in the horizontal load due to the increase in the amplitude (%Δm) at 40.0%, but flattening tends to occur when it moves towards 100.0%. Meanwhile, the tensile loading curve shows a significant improvement in the horizontal load up to 40.0% amplitude as well as a slight increase and tendency to flatten out at 100.0%. This condition indicates a decrease in the strength of the specimen up to the final stage of the experiment at an amplitude of 120.0%, and the hysteresis loops curve produced was observed to have a low slope pattern.

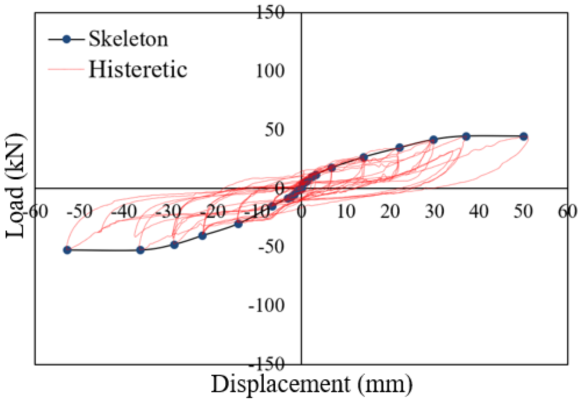

Fig. 6 Load vs. displacement for WTI

The maximum push load achieved was 44.88 Mpa, while the maximum pull load was 52.30 MPa. It was also clearly observed in Figure 7 that the rate of the initial push load was higher compared to the pull load by up to 20.0%, while the pull load was higher than the push load at the next loading stage.

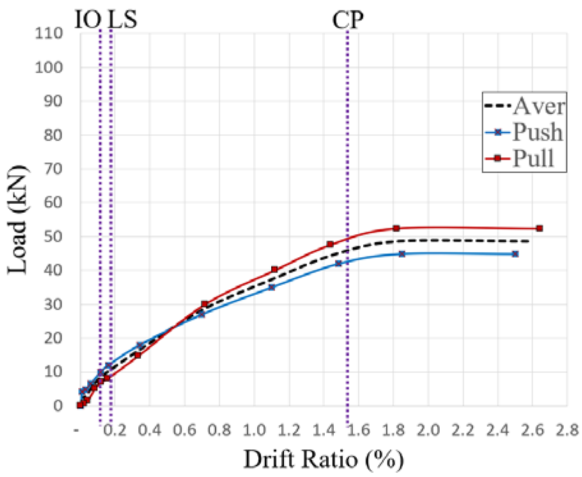

Fig. 7 Load vs. drift ratio for WTI

5.2 WTC Frame

Figure 8 presents the relationship of load to displacement due to the application of horizontal cyclic load on WTC in the form of hysteresis loop curves. In the push load, the curve was observed to have a significant increase up to 20.0% amplitude followed by an insignificant increase with the tendency to flatten up to 40.0%. In pull loading, the curve showed a significant increase up to 40.0%, followed by a significant increase and tendency to increase up to 60.0% in phase 3. This means the specimen decreased in strength up to the final stage of the test at an amplitude of 80.0% in phase 1, which is the maximum for the horizontal cyclic test used in this study. Moreover, the maximum push load achieved was 102.87 Mpa, while the maximum pull load was 80.09 MPa.

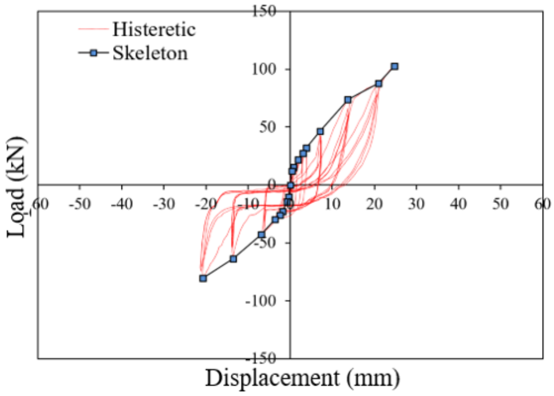

Fig. 8 Load vs. displacement for WTC

Figure 9 shows that the push load value that occurs on the specimen was always higher than the pull load in the initial loading up to 80.0%, which is the final stage of the horizontal cycle test.

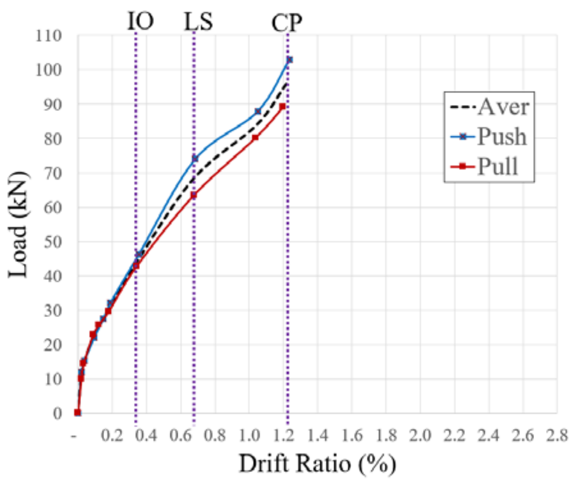

Fig. 9 Load vs. drift ratio for WTC.

5.3 Failure Mechanism of WTI

Figures 10, 11, and 12 show the stages of the failure mechanism in the WTI specimen for each building performance grade based on FEMA 356 standards. It was discovered that each grade of the structural performance has its range of load and drift ratios. Figure 10 shows that the structural performance grade IO started at cycle-2 with a drift ratio of 0.03% while the horizontal direction cracked in the interzone between the filler walls of the test object at a push load of 4.92 kN and a pull load of 1.38 kN. Meanwhile, the foam concrete did not develop cracks yet.

Figure 11 indicates that the structural grade LS occurred in cycle-4 to cycle-8 with a drift ratio ranging from 0.12% to 1.1%, thereby increasing the cracks in the walls of the specimen and the initiation of cracks in the columns as well as top and bottom beams at a push load around 10.00 kN – 35.00 kN and a pull load of 6.97 kN – 40.00 kN. It is important to note that vertical cracks occurred in some parts of the precast foam concrete used as infill walls in the WTI specimen.

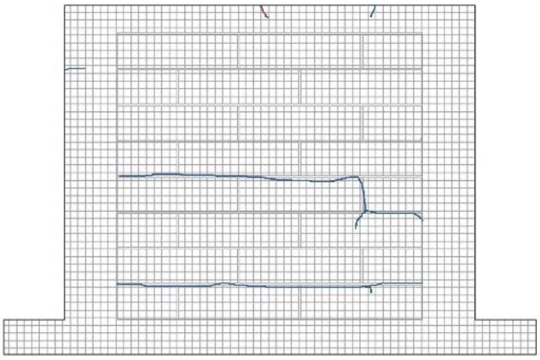

Fig. 10 Failure mechanism of WTI in IO grade

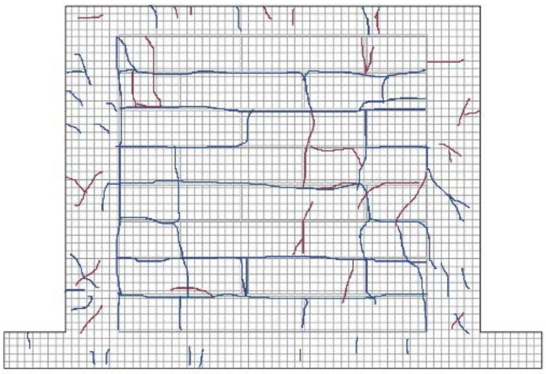

Fig. 11 Failure mechanism of WTI in LS grade

Figure 12 shows the structural performance grade CP in cycle-9 with a drift ratio of 1.49% and an increasing number of cracks in the walls of the specimen, beams, and columns, as well as the occurrence of cracks in the plastic joints at push loads of 42.00 kN and pull loads of 47.50 kN. The test ended on cycle-11 at a push horizontal load of 44.88 kN and a pull load of 50.00 kN with a drift ratio of 2.5%. The vertical cracking in the precast foam concrete was found to have increased at the maximum load test, but it was not as much as in the bed joint or mortar, as indicated in Figure 13.

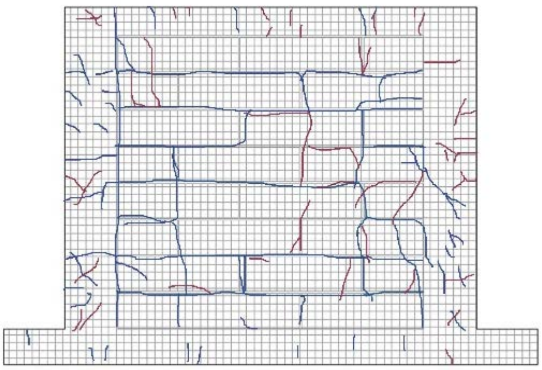

Fig. 12 Failure mechanism of WTI in CP grade

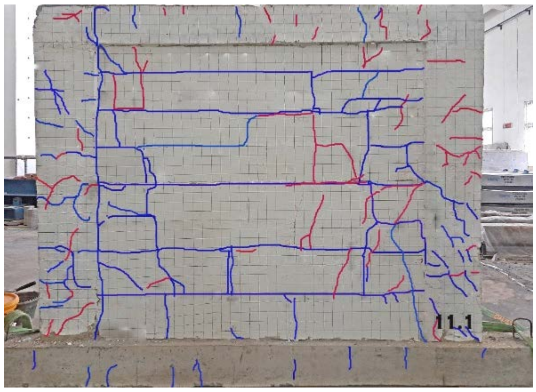

Fig. 13 Visual condition of WTI in CP grade

5.4 Failure Mechanism of WTC

Figures 14, 15, and 16 show the failure mechanism in the WTC frame for each grade of building performance. Figure 14 shows that the grade IO began at cycle 6 with a drift ratio of 0.36% and the appearance of hairline cracks on the precast foam concrete used as an infill wall at a push load of 46.34 kN and a pull load of 39.10 kN. In Figure 14, the grade LS occurred during cycle 7 to cycle 8 with a drift ratio of 0.69% to 1.05%, an increase in the number of cracks in the walls, columns, and beams, as well as the initiation of debonding on the CFRP sheet at a push load of 78.33 kN to 87.81 kN and a pull load of 71.40 kN to 80.10 kN. It is pertinent to state that several cracks appeared in the horizontal direction of the precast foam concrete, particularly around the CFRP strips. Meanwhile, Figure 15 shows the occurrence of grade CP during cycle 9 with a drift ratio of 1.24%, an increase in the cracks in the walls, beams, and columns, as well as debonding in 35% of the CFRP sheets at a push load of 102.87 kN. The test was terminated at cycle 9, but continuous cracking was observed in the precast foam concrete in a horizontal direction around the CFRP strip. Moreover, the foam concrete was detached, specifically at the CFRP attachment, when it occurred. The visual conditions of the WTI frame at the final stage of the horizontal cyclic test are displayed in the following Figure 17.

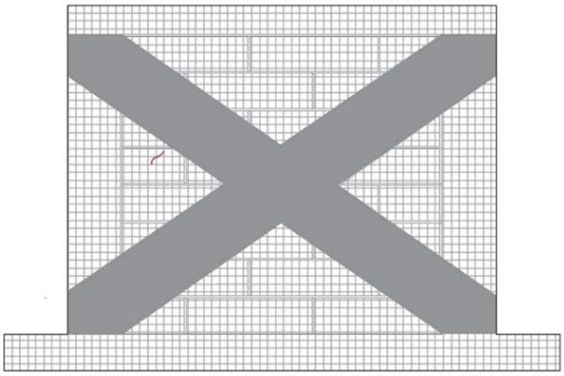

Fig. 14 Failure mechanism of WTC in IO grade

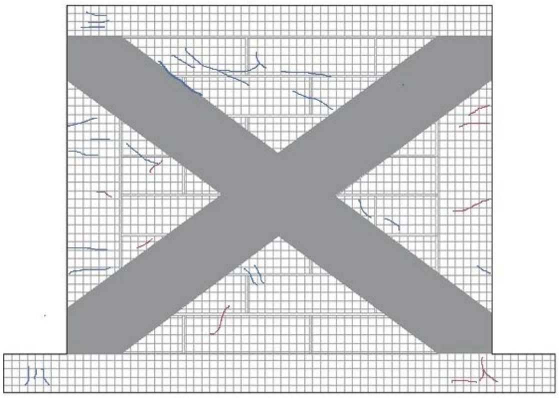

Fig. 15 Failure mechanism of WTC in LS grade

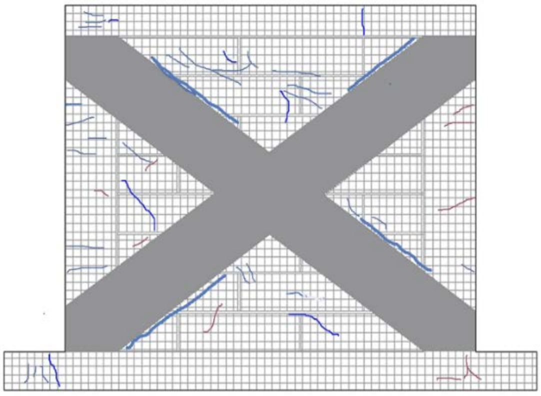

Fig. 16 Failure mechanism of WTC in CP grade

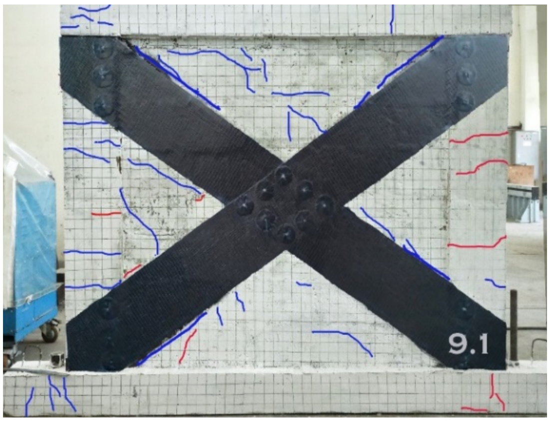

Fig. 17 Visual condition of WTC in CP grade

Table 6 shows the results of the strength ratio calculated for WTC and WTI specimens at each of their structural performance grade, including IO, LS, and CP, in order to determine the effectiveness of diagonal CFRP with a width of 36 cm applied to improve the horizontal strength of the specimen. It was observed that the peak load supported by the WTC specimen at the IO grade was 7.22 times greater than the WTI specimen, while the value at the LS grade was 2.11 and the CP grade was 2.99.

Table 6 The strength ratio of WTC to WTI

Structural Performance Grade (FEMA 356)	Load WTI (kN)	Load WTC (kN)	$\frac{GWTC}{GWTI}$
IO	6.42	46.34	7.22
LS	35.00	73.90	2.11
CP	44.88	102.87	2.29

6. CONCLUSIONS

The results from the data analysis and discussion showed that:

1. The specimen's maximum horizontal strength was raised by retrofitting CFRP.
2. The precast foam concrete specimens with the CFRP retrofitting underwent shear failure, which started with the CFRP sheets coming unglued and finished with shear structural collapse.
3. The infill wall had diagonal fissures with shear collapse, and the force pushing against it caused an in-plane failure.
4. The evaluation of the failure causes utilizing FEMA 356 revealed that CFRP has the capacity to impede damage to the specimen's IO, LS, and CP structural performance grades.

7. REFERENCES

[1] Altin S., Anıl O., Kara M.E., Kaya M. An experimental study on strengthening of masonry infilled RC frames using diagonal CFRP strips. Compos Part B: Eng., 2008, 39, pp 680–93.

[2] Magenes, G., and Calvi G. M. In-Plane Seismic Response of Brick Masonry Walls Earthquake Engineering And Structural Dynamics, 1997, Vol. 26, pp. 1091- 1112.

[3] Tomaževič M., Lutman M., Petković L. Seismic behavior of masonry walls: experimental simulation. J Struct Eng ASCE 122(9), 1996, pp. 1040–1047.

[4] Cai, G., dan Su, Q. Effec t of Infill on seismic performance of reinforced concrete frame structures - A full scale experimental study. Journal Of Earthquake Engineering. DOI: 10.1080/13632469, 2017, pp. 1387194.

[5] Dolsek M., Fajfar P. The effect of masonry infill on the seismic response of a four-storey reinforced concrete frame a deterministic assessment. Eng Struct, 2008, 30, pp 1991–2001.

[6] Hashemi A., Mosallam K.M. Shake-table experiment on reinforced concrete structure containing masonry infill wall. Earthquake Eng Struct Dyn, 2006; 35, pp. 1827–52

[7] Mansyur M., Tjaronge M.W., Irmawaty R., Amiruddin A.A. (2022). Performance of Prefabrication Foam Concrete as Infill Wall Under Cycle Horizontal Loading. International Journal of Engineering Vol 35, No.02, 2022, pp. 337-343.

[8] Tumpu, M., Parung H., Tjaronge M.W., Amiruddin A.A. Failure Pattern of Prefabrication Foam Concrete as Infill Wall Under In-Plane Lateral Loading. Design Engineering, No. 07, 2021, pp. 7158-7176.

[9] Sunarno Y., Tjaronge M.W., Irmawaty R. (2020). Preliminary Study on Early Compressive Strength of Foam Concrete using Ordinary Portland Cement and Portland Composite Cement. IOP Conference Series: Earth and Environmental Science. Vol 419, No. 1 012033. Doi 10.1088/1755-1315/419/I/012033.

[10] Syahrul, Tjaronge M.W., Djamaluddin R., Amiruddin A.A. Flexure Behavior of Normal and Lightweight Concrete Composite Beams. Civil Engineering Journal, Vol. 7 No. 2, 2021, pp. 549-559, Doi: 10.28991/cej-2021-13091673.

[11] Amran Y.H.M., Farzadnia N., and Ali A. Properties and Application of Foam Concrete, a review. Construction and Building Material, Vol 101, 2015, pp. 990-1005. Doi:10.1016/j.conbuildmat.2015.10.112.

[12] Mertoglu C., Anil O., Durucan C. Bond slip behavior of anchored CFRP strips on concrete surfaces. Construction and Building Materials. 123,2016, pp. 553–564. https://doi.org/10.1016/j.conbuildmat.2016.07.060.

[13] Chagnon N., Massicotte B. Seismic retrofitting of rectangular bridge piers with CFRP, ConMat'05 Third International Conference on Construction Materials: Performance, Innovations and Structural Implications, 2005, pp. 1–10.

[14] Teng J. F., Chen J.F., Smith S.T., Lam L. (2002). FRP-Strengthened RC Structures, Wiley, Chichester.

[15] Chen J.F., Teng J.G. Anchorage strength models for FRP and steel plates bonded to concrete, J Struct. Eng. ASCE 127 (7) ,2001, pp. 784–791.

[16] Smith S.T., Teng J.G. FRP-strengthened RC beams-I: review of debonding strength models, EngStruct 24 (4), 2002, pp. 385–395.

[17] Smith S.T., Teng J.G. FRP-strengthened RC beams-II: assessment of debonding strength models, EngStruct 24 (4), 2002, pp. 397–417.

[18] Smith S.T., Teng J.G. Shear-bending interaction in debonding failures of FRP-plated RC beams. Adv. Struct. Eng. 6 (3), 2003, pp. 183–199.

[19] FEMA 356. Pre standard and commentary for the seismic rehabilitation of buildings. ASCE, Federal Emergency Management Agency, 2000.

[20] ASTM E 2126-02a. Standard Test Methods for Cyclic Load Test for Shear Resistance of Framed Walls for Buildings, 2002.

[21] ASTM C39. Standard Test Method for Compressive Strength of Cylindrical Concrete Specimens, 2012.

[22] ASTM C780. Standard Test Methods for Preconstruction and Construction Evaluation of Mortars for Plain and Reinforced Unit Masonry, 2020.

[23] ASTM D3039. Tensile Testing for Advanced Composite Materials, 2014.

[24] ASTM D790. Standard Test Methods for Flexural Properties of Un-reinforced and Reinforced Plastics and Electrical Insulating Material, 2017.

[25] SNI 1726-2019. Tata cara Perencanaan Ketahanan Gempa untuk Struktur bangunan gedung dan non gedung, 2019. (Procedure for Earthquake Endurance Planning for Building and Non-Building Structures) (In Indonesian).